ACCOUNTS of chemical research

pubs.acs.org/accounts Article

Single Atom Dynamics in Chemical Reactions

Edward D. Boyes,* Alec P. LaGrow, Michael R. Ward, Robert W. Mitchell, and Pratibha L. Gai*

Cite This: *Acc. Chem. Res.* 2020, 53, 390−399 Read Online

ACCESS | Metrics & More | Article Recommendations

CONSPECTUS: Many heterogeneous chemical reactions involve gases catalyzed over solid surfaces at elevated temperatures and play a critical role in the production of energy, healthcare, pollution control, industrial products, and food. These catalytic reactions take place at the atomic level, with active structures forming under reaction conditions. A fundamental understanding of catalysis at the single atom resolution is therefore a major advance in a rational framework upon which future catalytic processes can be built. Visualization and analysis of gas-catalyst chemical reactions at the atomic level under controlled reaction conditions are key to understanding the catalyst structural evolution and atomic scale reaction mechanisms crucial to the performance and the development of improved catalysts and chemical processes. Increasingly, dynamic single atoms and atom clusters are believed to lead to enhanced catalyst performance, but despite considerable efforts, reaction mechanisms at the single atom level under reaction conditions of gas and temperature are not well understood. The development of the atomic lattice resolution environmental transmission electron microscope (ETEM) by the authors is widely used to visualize gas−solid catalyst reactions at this atomic level. It has recently been advanced to the environmental scanning TEM (ESTEM) with single atom resolution and full analytical capabilities. The ESTEM employs high-angle annular dark-field imaging where intensity is approximately proportional to the square of the atomic number (Z). In this Account, we highlight the ESTEM development also introduced by the authors for real time in situ studies to reliably discern metal atoms on lighter supports in gas and high temperature environments, evolving oxide/metal interfaces, and atomic level reaction mechanisms in heterogeneous catalysts more generally and informatively, with utilizing the wider body of literature. The highlights include platinum/carbon systems of interest in fuel cells to meet energy demands and reduce environmental pollution, in reduction/oxidation (redox) mechanisms of copper and nickel nanoparticles extensively employed in catalysis, electronics, and sensors, and in the activation of supported cobalt catalysts in Fischer−Tropsch (FT) synthesis to produce fuels. By following the dynamic reduction process at operating temperature, we investigate Pt atom migrations from irregular nanoparticles in a carbon supported platinum catalyst and the resulting faceting. We outline the factors that govern the mechanism involved, with the discovery of single atom interactions which indicate that a primary role of the nanoparticles is to act as reservoirs of low coordination atoms and clusters. This has important implications in supported nanoparticle catalysis and nanoparticle science. In copper and nickel systems, we track the oxidation front at the atomic level as it proceeds across a nanoparticle, by directly monitoring Z-contrast changes with time and temperature. Regeneration of deactivated catalysts is key to prolong catalyst life. We discuss and review analyses of dynamic redox cycles for the redispersion of nickel nanoparticles with single atom resolution. In the FT process, pretreatment of practical cobalt/silica catalysts reveals higher low-coordination Co^0 active sites for CO adsorption. Collectively, the ESTEM findings generate structural insights into catalyst dynamics important in the development of efficient catalysts and processes.

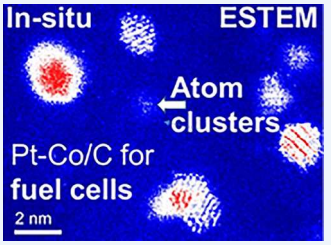

INTRODUCTION

Many heterogeneous chemical reactions involve gases catalyzed over solid surfaces at elevated temperatures and play a critical role in the production of energy, healthcare, pollution control, industrial products, and food.[1−3] The dynamic heterogeneous gas−solid catalyst reactions take place at the atomic level, and active catalyst structures may form only under reaction conditions. Supported nanoparticles are used extensively as heterogeneous catalysts, and they contain metal particles of variable sizes dispersed on supports such as ceramic oxides and carbon. Nanoparticle catalysts have been shown to have numerous advantages over their bulk counterparts due to their high surface to volume ratios and size dependent properties.[1−3]

Insights into the complex catalytic reactions at the atomic level are crucial to understanding and controlling fundamental reaction mechanisms and atomic scale structure−property relationships to develop improved materials and processes. Direct dynamic in situ studies under controlled reaction environment conditions of gas and high temperature play a key role in understanding them and in situ environmental electron microscopy is increasingly utilized for studying and analyzing

Received: September 22, 2019
Published: February 5, 2020

https://dx.doi.org/10.1021/acs.accounts.9b00500
Acc. Chem. Res. 2020, 53, 390−399

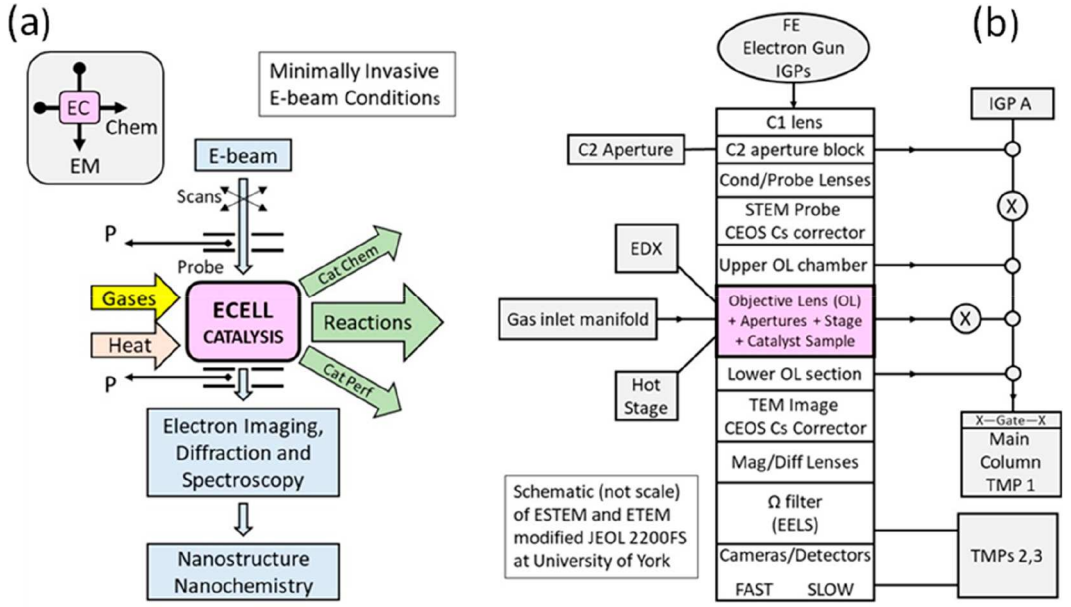

Figure 1. (a) Schematic of the ESTEM concept and functionalities. In the ESTEM (and ETEM), the EM column shares a catalyst sample with gas environment chemical reactor (ECELL). EC is the ECELL, with reaction providing products, catalyst nanostructure, and chemical basis of performance. (b) Schematic related to JEOL 2200FS platform employed for the pioneering double aberration corrected ESTEM/ETEM system at York. The apertures and differential pumping with pressure zones sustain continuous gas pressures around the sample in the Pa to mbar ranges.

how catalysts behave under simulated reaction conditions. Direct real time observation of nanostructural evolution under dynamic reaction conditions in situ with an atomic resolution environmental transmission electron microscope (atomic resolution ETEM) is a powerful scientific tool in the chemical and materials sciences for nanostructure dependent data.[4−9] These data often cannot be obtained directly by other means.

Increasingly, single atoms and atom clusters are believed to lead to enhanced catalyst performance, supported by EM studies in vacuum and theoretical modeling.[10−18] Single atom species and small clusters are especially important for catalysis applications due to their low surface coordination numbers and high surface area, which can potentially lead to more active sites to bind reagents.[12,18] In nanoparticle catalysts, particle sintering leads to the loss of surface area and performance of the nanoparticles.[19] It is therefore important to observe and analyze, in real time, single atom interactions with nanoparticles in supported nanoparticle systems to gain insights into atomic scale reaction mechanisms.

Single atoms, including in supported metal nanocatalysts, have been viewed in the high vacuum environment of an electron microscope at room temperature (RT) or higher temperatures using methods that include high angle annular dark field (HAADF) imaging in the scanning TEM (STEM).[20−22] In HAADF imaging for atomic number (Z)-contrast, electrons that undergo high angle Rutherford scattering in electron beam-sample interactions are collected and the image intensity is approximately proportional to Z^2.[20,23] Whereas in the TEM, the image contrast, including for supported systems,[24] is dominated by diffraction and phase effects which can make it difficult to reliably discern atomic features on supports. Aberration correction for electron lenses[25] and methods to identify single atoms[21] are reported in the literature.

In situ visualization and analysis of reacting single atoms reliably in controlled gas and temperature environments in real-time have been lacking, leading to insufficient understanding of reaction mechanisms in chemical reactions at the single atom level. In this Account, we consider single atom dynamics in chemical reactions in reacting gas and temperature environments, exploring reaction mechanisms at the fundamental atom level and their role in the reactions.

The atomic resolution ETEM design and development pioneered by Boyes and Gai[4] for visualizing and analyzing gas−solid catalyst reactions at the atomic level under controlled gas and temperature environments is used by EM manufacturers[26] and in laboratories globally.[27−33] The ETEM invention is also outlined.[9] The atomic resolution ETEM development[4] with a gas-in-microscope design (with pressures of many mbars and temperatures up to 1000 °C or higher) incorporates the integrated EM sample chamber as the chemical reactor and radial holes in the objective lens polepieces for gas.[4] It is thus a major change from the conventional vacuum methods and the earlier lower resolution environmental EM methods with ex situ reactor cells inserted into the EM. The gas-in-microscope method is extensively used, whereas TEM gas holder technology is still evolving regarding resolution and analytical sensitivity.

To visualize and analyze single atom dynamics reliably in chemical reactions in situ, in real time, an environmental scanning TEM (ESTEM) with single atom resolution and key additional analytical capabilities has been designed and constructed.[34−36] This extends and advances the original atomic resolution ETEM.[4] Further, both the ESTEM and ETEM (referred to as E(S)TEM) capabilities have been incorporated in the same instrument, described below.

■ ANALYTICAL SINGLE ATOM RESOLUTION-ESTEM DEVELOPMENT

Dynamic in situ experiments in the electron microscope benefit from aberration correction (AC) to provide a series of unique single images, each at optimal and minimal defocus,

https://dx.doi.org/10.1021/acs.accounts.9b00500
Acc. Chem. Res. 2020, 53, 390−399

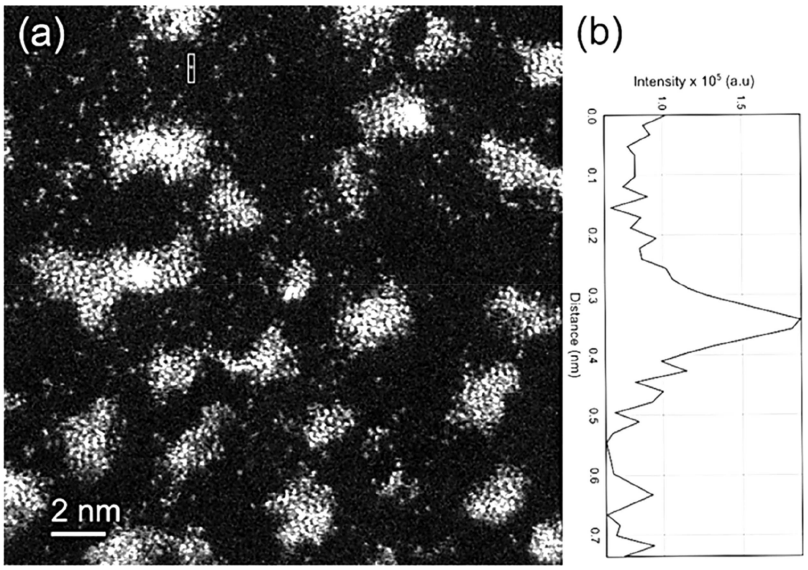

Figure 2. (a) Single atoms in Pt/C catalyst in ESTEM-HAADF. (b) Intensity profile of a single atom in (a) marked in the top left-hand corner; single atoms are about 100 pm.

with a continuous range of faithfully recorded spatial frequencies; rather than requiring an impractical multi-image through-focal series.

A double aberration corrected (Schottky) FEG TEM/STEM (JEOL 2200 FS) at 200 kV is innovatively modified to provide both the ETEM[34] and, for the first time, ESTEM full functionalities.[35,36] These include introducing controlled reaction conditions of continuously flowing gas environments and temperatures controlled with a MEMS heating stage from DENSsolutions, with uncompromised HAADF *Z*-contrast ESTEM imaging with single atom resolution, low background energy dispersive X-ray spectroscopy (EDX), electron energy loss spectroscopy (EELS) for chemical analysis, and wide-angle dynamic electron diffraction (ED) analyses of nanoparticle structures during reactions. The new permanently mounted environmental cell (ECELL, or gas reaction cell) developments retain and enhance the full performance of the original core instrument with single atom sensitivity in imaging during chemical reactions.[35−37] The open-aperture gas-in-microscope instrument has differentially pumped column sections separated by repurposed and additional fixed beamline apertures and a new pumping system, shown in Figure 1.

In addition to providing direct and unparalleled insights into the evolution of dynamic atomic structural changes under controlled reaction conditions, the E(S)TEM allows the detection, in real time, of surface as well as subsurface structural phenomena important in many chemical reactions. These include access to metastable states during the reaction, changes in structures, chemical composition and oxidation states, surface and subsurface diffusion of reacting species, active sites on specific catalyst surfaces for binding gas molecules influencing reaction mechanisms, and interactions between single atoms and nanoparticles. Key pathways of catalyst activation, operation, and aging can be studied in a variety of gas pressures and temperatures to understand kinetics and reaction processes. The studies are central to enabling smarter synthesis procedures and improved catalysts and processes.

To ensure minimally invasive electron beam damage, to control secondary effects such as contamination and generally to avoid introducing additional change processes not connected to the real chemical catalysis, the electron dose has to be controlled. Careful calibration procedures are therefore employed to avoid possible deleterious effects of the electron beam. Blank calibration in situ experiments are carried out by beam blanking. The beam is blanked during reaction experiments to minimize sample exposure to the beam, and particles are only exposed to the beam during data setup, interval examinations, and actual data acquisition.[24,34−39] To probe the effect of the beam on particle sintering, regions with no previous exposure to the electron beam are also imaged periodically. The data are checked with in situ experiments under the same reaction conditions using low dose beam currents[40] and using different marks to space beam-on/off ratios.

High resolution ESTEM data of reaction processes are recorded primarily at image magnifications of 8−12MX with 512 or 1024 line frames and pixel dwell times of 19 or 38 μs, using 50 Hz synchronization. The inner and outer collection angles of the STEM HAADF detector are 110 and 170 mrad, respectively, and the incident probe has a calibrated convergence semiangle of 24 mrad. Videos are made with reduced frame times and lower pixel counts to analyze and illustrate the dynamic and often competitive nature of the processes. Gas pressures (of a few Pa) cover sample surfaces with thousands of monolayers of gas per second. This is generally fully adequate[35] to flood the surface with gas molecules and to drive the chemistry under conditions defined in surface science as "high pressure".[41] Analyses of solid state reaction mechanisms in the EM reactor show that the mechanisms are consistent with those in technological reactors employing many bars of gas pressure.[7,8] Quantitative-STEM (QSTEM)[42] image simulations are also performed and compared with experimental data to provide insights into nanostructures.[38−40,43]

SINGLE ATOM DYNAMICS IN CHEMICAL REACTIONS USING ESTEM

Single atom dynamics as a function of gas and temperature are of great importance in heterogeneous catalytic chemical

https://dx.doi.org/10.1021/acs.accounts.9b00500
Acc. Chem. Res. 2020, 53, 390−399

reactions. In the following sections, we utilize recent experimental results to reveal single atom dynamics and atomic scale reaction mechanisms under controlled reaction conditions in catalysts of interest in fuel cells, energy and environment.

Recent in situ ESTEM studies under controlled reaction conditions have revealed reaction mechanisms and explain the performance of a number of catalysts.[24,34−40,43,44] They have revealed single atoms and clusters of metal atoms on lighter supports in metal nanocatalysts operating under flowing gas environments and temperatures, evolving oxide/metal interfaces, and atomic mechanisms in heterogeneous catalysts for energy production. These include platinum nanocatalysts on carbon which are important in fuel cells and hydrogenation, dynamic reduction/oxidation (redox) mechanisms of copper and nickel nanoparticles employed in catalysis, electronics, sensors, in the activation of catalysts for Fischer−Tropsch (FT) synthesis to produce fuels, and bimetallic catalysts of interest in economical fuel cell technology for controlling environmental pollution.

Single atoms show up as white dots on lower-Z supports in the in situ ESTEM-HAADF images presented here. Figure 2a shows single atoms and clusters of a model Pt sample sputtered on to a carbon support, with the image intensity profile of a single atom. The very thin (1−2 atoms high), raftlike clusters are made up primarily of partially ordered {111} spacings with a general ⟨110⟩ texture. The image clarity enables a better structure−function correlation.

Supported Nanoparticles

Single atom dynamics and nanoparticle sintering in Pt/C catalysts of interest in fuel cells as a function of hydrogen gas and temperature using the ESTEM have been described.[35,36] By directly monitoring the dynamic hydrogen reduction process at operating temperatures in a model Pt/C catalyst, Pt atom migrations from irregular nanoparticles (NPs) and the resulting faceting are observed, which are shown in Figure 3.

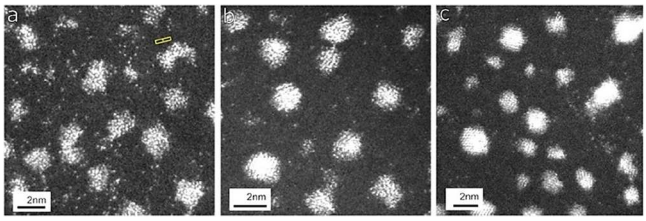

Figure 3. Dynamic ESTEM imaging of Pt/C catalyst at single atom resolution in hydrogen gas as a function of temperature: (a) RT with single atoms detected between Pt NPs; (b, c) increased faceting of NPs in H_2 at 400 and 500 °C, respectively. (Scale bar = 2 nm.)

Figure 3a shows dynamic ESTEM imaging in 2 Pa hydrogen gas at RT. An extensive population of single atoms is detected on the support between the Pt NPs, and the development of 3D particle forms, with some faceting, is observed in the gas even at RT; (b) single atoms between more faceted Pt NPs are observed at 400 °C in the gas and (c) in hydrogen gas at 500 °C, where clusters and increased faceting of the nanoparticles are observed, with fewer single atoms detected on the support than in (a) and (b).

Figure 4 shows illustrative data of normalized ESTEM-HAADF intensities.[35] The arrow inside the box in (a) indicates single-atom migration and dynamics, providing analysis of small particle shapes atom-by-atom in the ESTEM.

Dynamic migration of single atoms from irregular nanoparticles (e.g., P) from the same area and increased faceting of the nanoparticle during the reaction are illustrated in Figure 5, taken at intervals of 0.335 s.

In hydrogen environments, low coordination surface atoms are replaced by surface facets through local rearrangements to minimize the particle surface energy. The observations indicate that the irregular nanoparticles primarily act as a source of potential adatoms and clusters, providing new insights into the role of nanoparticles in chemical catalytic reactions.[24,35−37] The observations and analyses further reveal how surface faceting of particles evolves in the nanocatalyst system. Through the use of a support material with an abundance of anchoring sites, migrating atoms can be stabilized to provide further active sites for adsorption, with the nanoparticles acting as reservoirs and recipients of adatoms and migratory clusters.[36]

Effect of Pretreatment of Catalysts in Fischer−Tropsch Synthesis for Fuels

Fischer−Tropsch (FT) catalysis is a major industrial process for converting syngas (hydrogen and CO) to transportation fuels and other hydrocarbons.[45−49] The process generally uses oxide supported cobalt catalysts. Despite considerable literature on the FT process, the effect of pretreatment (activation) in hydrogen on the catalysts is not well understood. Effects of pretreatment of both dried, reduced (D), and dried calcined reduced (DC) supported real-world (practical) cobalt (Co) catalyst precursors on various supports such as SiO_2, TiO_2, ZrO_2, and Al_2O_3 have been visualized and analyzed using E(S)TEM with single atom resolution, and complemented by chemical methods, including extended X-ray absorption fine structure (EXAFS), X-ray absorption spectroscopy (XAS), and diffuse reflectance infrared Fourier transform spectroscopy (DRIFTS).[44] The methods have played a key role in unlocking mysteries of the activation process in FT catalysis, including cobalt dispersion, the presence of cobalt nanoparticles with face-centered cubic (fcc) and hexagonal close packed (hcp) phases, the dynamic atomic structure and the activity of the catalysts. The ESTEM is used for tracking single atom dynamics in the activation of cobalt/silica catalysts used for the FT process.[44] In D samples, Co atom dynamics, the presence of a large number of Co single atoms and clusters are revealed with Co nanoparticles, as shown in Figure 6a and b, recorded at 2 min intervals. In DC samples, the ESTEM reveals the presence of large Co-oxide agglomerates near Co nanoparticles and clusters (c and d). Correlation of the nanostructure with the FT catalytic activity reveals higher activity for D, with the ratio of the relative activity for D/DC of 1.6, indicating that the dynamic active species with Co^0 atoms, clusters and small NPs of Co play a pivotal role in the CO adsorption and enhancing the catalyst performance.[44]

The findings have revealed that D samples are more active than the DC samples, irrespective of the support employed with no change to the selectivity values. Systematic ESTEM and parallel catalytic activity studies of D and DC samples have revealed higher activity of D corresponding to a better dispersion of Co active species and a greater ratio of hcp to fcc Co phases.[44] The ESTEM findings further show that the calcination process in DC samples leads to larger Co particles and cobalt-oxide agglomerates, which reduce the surface area

https://dx.doi.org/10.1021/acs.accounts.9b00500
Acc. Chem. Res. 2020, 53, 390−399

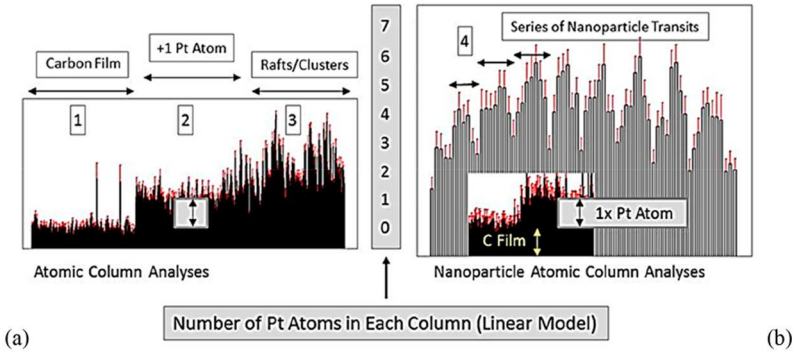

Figure 4. Plots of ESTEM HAADF intensities normalized to single Pt atom contrast (region marked 2, above background (1)) for atomic column height analyses across (a, left graph): as deposited single atom layers (2), clusters and rafts (3) on the unheated carbon support film (1) at ambient temperature (25 °C); and (b, right graph) in transits across a multiatom thick 3D crystalline nanoparticles of 1.5−2 nm (4) after exposure and crystallization under hydrogen atmosphere at 500 °C for 30 min and analyzed under those conditions.

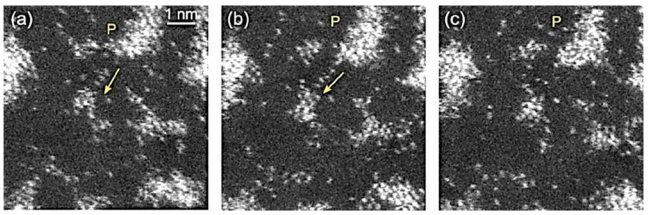

Figure 5. Single atom dynamics in reacting Pt/C catalysts with migration of single atoms, (indicated at the arrows in (a) and (b), and from particle P), leading to increased faceting (crystallization) of the particle and clusters in (c).

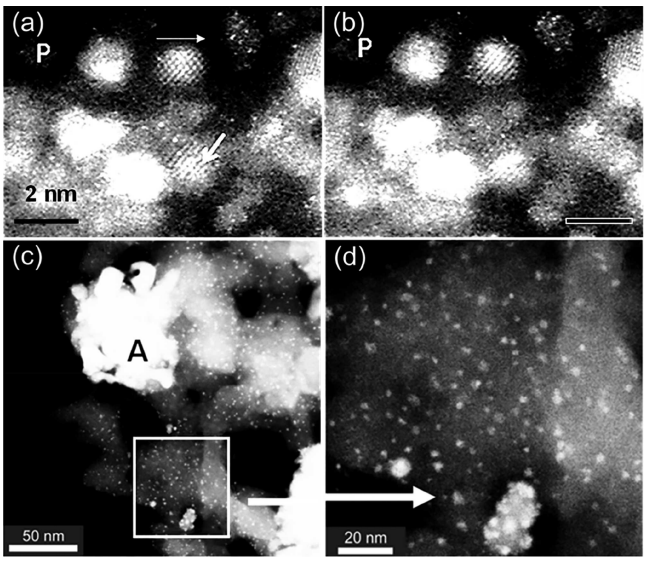

Figure 6. Dynamic ESTEM-HAADF image sequence as a function of time in hydrogen at 400 °C. Images in (a) and (b) are from the same area near P: (a) practical D-Co/SiO2 catalyst, showing Co single atoms (about 100 pm), clusters (indicated at top thin arrow), and NPs and (b) tracking of the atoms, clusters, and NPs. (Scale bar = 2 nm.) (c) DC-catalyst, showing primarily Co-oxide agglomerates (e.g., at A) and Co NPs. (d) Square area in (c) enlarged.

and the number of active sites available for CO adsorption. Based on the ESTEM and chemical data, removal of the calcination process results in improved activity of the supported catalysts. The dynamic ESTEM observations have revealed more highly dispersed Co metal species (Figure 6a and b), in reacting D samples, leading to smarter pretreatment synthesis methods with more active sites for CO adsorption in FT catalysis.

VISUALIZING METAL/OXIDE INTERFACE TRANSITION IN NANOPARTICLES

Understanding reduction−oxidation (redox) mechanisms in catalytically active transition metal nanoparticles is key to improving their applications in a variety of chemical processes. Significantly, in some important metal systems, including copper, the contrast of the important oxide/metal interface is difficult to distinguish by conventional TEM methods. Copper is used in its metallic and oxidized forms for applications in electronics, sensors and in methanol synthesis catalytic technology as part of the copper, alumina, and zinc oxide system.[50,51] A fundamental understanding of the redox mechanisms of copper is therefore of critical importance to improving catalytic performance and corrosion control, and in other technological applications.

In copper systems by directly following time-resolved dynamic oxidation processes in situ in real time, controlled ESTEM conditions ideal to distinguish the metal and the oxide are used. The ESTEM observations shown in Figure 7 track the oxidation front at the atomic level, as it progresses across a copper nanoparticle, by directly monitoring the changes in the Z-contrast as a function of time in an oxygen environment at the operating temperature of 500 °C (Figure 7A).[38] The evolving surface structure reveals that the oxidation occurs via the nucleation of the oxide phase (Cu_2O) from one area of the nanoparticle which progresses unidirectionally across the particle. This process can be reversed with the same dynamics during reduction with the Cu nucleating from the Cu_2O and the interface between the two moving across the particle over the course of the reduction (Figure 7B) and repeated multiple times. The Cu-to-Cu_2O interface is stabilized by the relationship of Cu{111}//Cu_2O{111} as shown in Figure 7C (with either the 7 × 6 or 6 × 5 lattice matching relationships, or a mixture of the two).[38]

The oxidation reaction is observed to be reversible in hydrogen at the atomic level and occurs in a similar way, although the wetting angle between the copper and its oxide is much lower, creating a protrusion off the particle to minimize the interface size, with island formations occurring at 300 °C in hydrogen. The wetting angle is increased at higher temperatures (400 and 500 °C) during the reduction, minimizing the

https://dx.doi.org/10.1021/acs.accounts.9b00500
Acc. Chem. Res. 2020, 53, 390−399

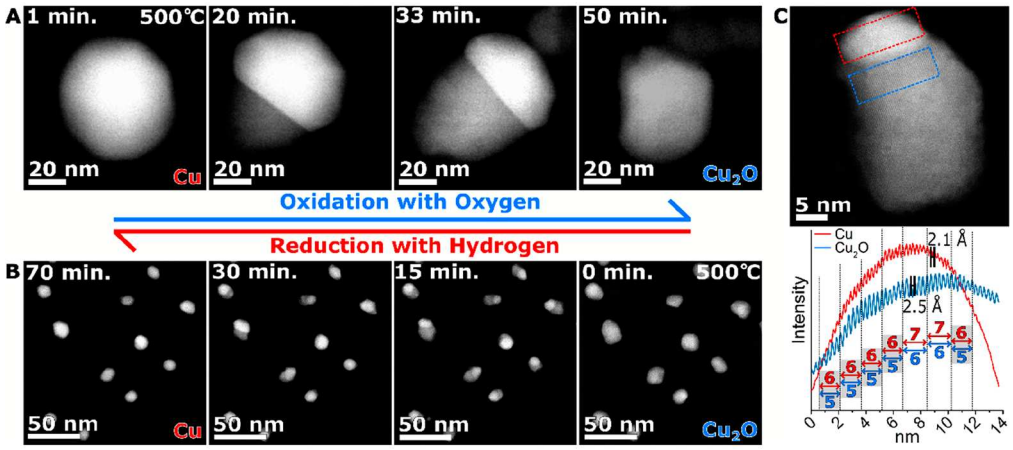

Figure 7. Dynamic ESTEM-HAADF of (A) the dynamic oxidation sequence of Cu as a function of time, at 500 °C in 2 Pa oxygen gas and (B) the dynamic reduction sequence of Cu_2O at 500 °C in 2 Pa hydrogen gas shown as a function of time in reverse order to illustrate the redox cycle. (C) Cu/Cu_2O nanoparticle at atomic resolution illustrating the contrast variation between the metal (top) and the oxide (bottom), with the interface revealed and the lattice matching behavior noted in the graph below with the red intensity profile coming from the red dashed box and the blue lines from the blue dash box.

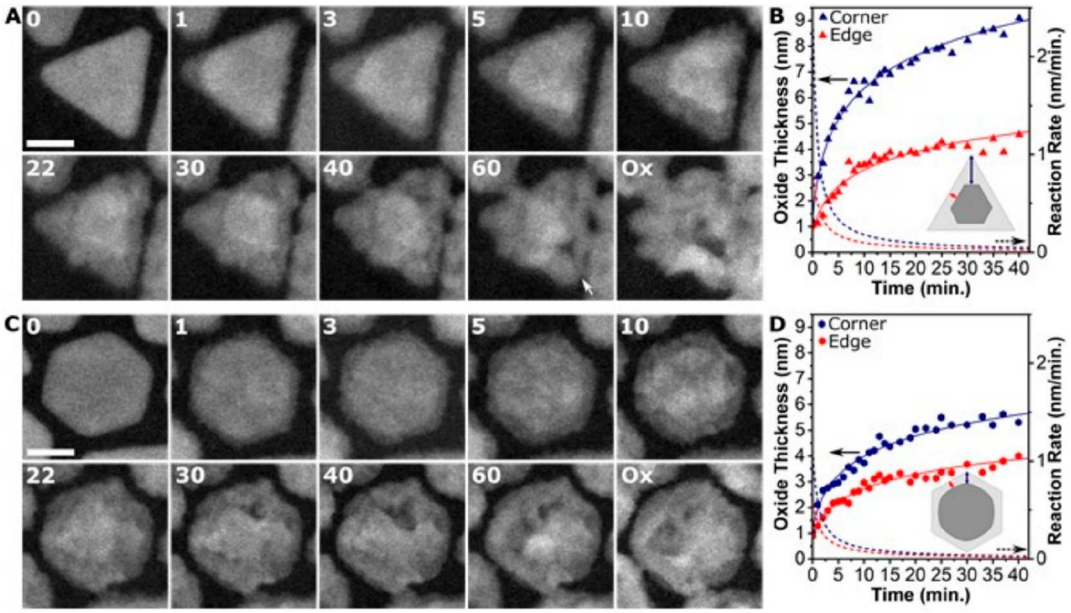

Figure 8. In situ visualization and analysis of dynamic oxidation of shape-controlled nanoparticles in ESTEM-HAADF. (A) Triangular plate (T, with 22 nm in size) and (C) hexagonal plate (H, 22 nm) at 400 °C in 2 Pa oxygen gas. (B, D) Graphs of the averaged oxide thickness (x) over time (in mins) for the (B) T and (D) H plates with the fits shown by the solid line. The derivative of the fit (dx/dt) giving the reaction rate is indicated by the dashed line. The insets illustrate thickness measurements.

extent of protrusion of the copper phase. The in situ observations of the faster oxidation of copper metal and the slower reduction of the oxide show that the two processes are asymmetrical.[38] The findings provide a much deeper understanding of the redox processes at the atomic level and demonstrate the value of ESTEM-HAADF.

■ SHAPE-CONTROLLED NANOPARTICLES

By observing Z contrast changes in the ESTEM, site dependent oxidation kinetics could be followed in shape-controlled nanoparticles.[52] Ni-based systems are of interest in catalysis, alloy production, and energy applications. Icosahedra, decahedra, and triangular and hexagonal plates of nickel have been studied to understand their oxidation kinetics (Figure 8A). It is observed that in all cases the corner sites are oxidized more readily than the edge sites. The increased reactivity of the corners is proposed to be due to the corners having lower coordination numbers than the edges and therefore being more accessible to the incoming oxygen gas. The difference in the oxidation rates between the corners and the edges, shown in Figure 8B, remains until the oxide is several nanometers thick. This behavior is the most marked in the triangular plates where the shape anisotropy of the particles restricts the ability to reduce the coordination of atoms at the developing Ni/NiO interface and create a fairly circular metal core. The rate of oxidation is associated with the local atomic coordination at the interface and Ni^{2+} diffusion through the oxide shell until the Ni core becomes rounded leading to a steady-state oxidation rate, almost identical for all particle shapes (Figure 8B).

https://dx.doi.org/10.1021/acs.accounts.9b00500
Acc. Chem. Res. 2020, 53, 390−399

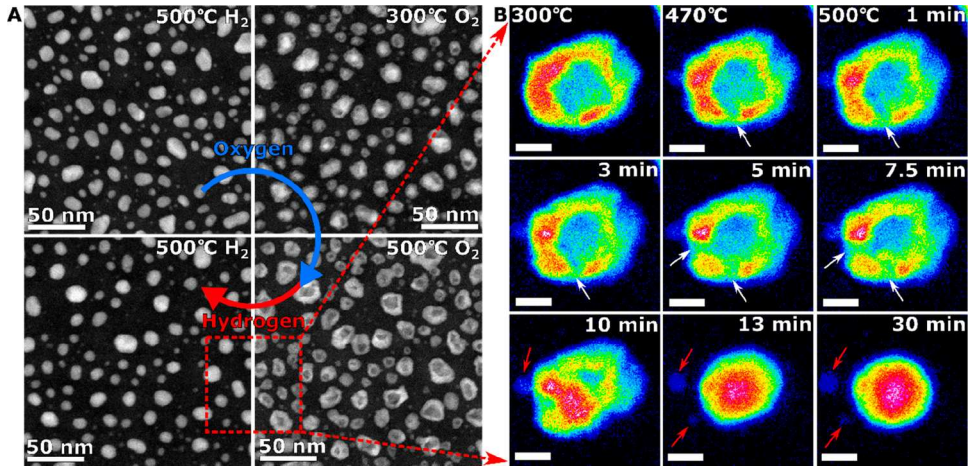

Figure 9. In situ ESTEM-HAADF images of (A) the transition from nickel to hollow nickel oxide with 2 Pa oxygen and back to nickel in the presence of 2 Pa hydrogen. (B) Single nanoparticle (NP) in the reduction of hollow NiO in 2 Pa hydrogen, with thermal colors showing intensity changes with time (from 1 to 30 min). White arrows point out where breaks occur in the NP shells. Small clusters/particles break away from the NP during reduction (e.g., at red arrows), and the grain movement is indicated by black arrows. Scale bars = 5 nm.

The dynamic observations reveal that larger particles and more anisotropic shapes require more time to rearrange the metal/metal oxide interface and therefore enhanced oxidation rates of the corner sites are retained for longer. The icosahedral nanoparticles are found to be the most corrosion resistant due to their isotropic structure, while the triangular plates are the least. The smaller nanoparticles (edge lengths less than ∼10 nm) have an induction period where the oxidation occurs preferentially at the corners before the edges begin to oxidize, and it seems most likely to occur due to oxygen diffusion along the particles surface to the most reactive parts of the nanoparticle.

Ni NANOPARTICLE CATALYST REDISPERSION VIA THE REDUCTION OF HOLLOW NiO

The effectiveness of industrial solid catalysts is typically reduced over time on stream through deactivation mechanisms and particularly the loss of surface area due to catalyst particle size increase by sintering.[53−57] Sintering mechanisms for nanoparticles include Ostwald ripening (OR) by atom migration from shrinking smaller particles to growing larger ones driven overall by surface energy considerations. The other main sintering mechanism is particle migration and coalescence (PMC). Processes to regenerate nanoparticle catalysts which have deactivated due to sintering or poisoning are commonly used to extend the economical life of catalyst effectiveness. Catalysts are designed to reduce deactivation by among other things tailoring particle-support interaction chemistry and geometry, and by controlling the initial nanoparticle size distribution. They can be regenerated by particle redispersion to reduce the effects of deactivation. An important approach to regenerate smaller more active nanoparticle catalysts is to employ reduction−oxidation (redox) cycles to redisperse the nanoparticles. However, insights into redox pathways of catalyst regeneration under reaction conditions at the atomic level are still limited.

In situ dynamic ESTEM-HAADF is important to visualize and analyze redox cycles of nickel nanoparticles to obtaining atomic level insights into their behavior and redispersion.[39] Cycling Ni/NiO system through successive redox cycles (Figure 9A) reveals that the regeneration of the smallest nanoparticles which disappear due to sintering processes, occurs by the ejection of small nickel particles (or clusters) during the reduction of hollow NiO nanostructures (Figure 9B). The studies have key implications for the regeneration of catalysts from materials that can oxidize to form hollow oxide structures such as Fe, Cu, Co, and Ni.

BIMETALLIC CATALYST PRECURSOR TRANSFORMATION FOR FUEL CELLS

To reduce pollution, combat climate change, and meet energy demands, fuel cells are seen as an alternative to using fossil fuels in transport applications.[58] Developing a cost-effective oxygen reduction catalyst for fuel cell electrodes is perceived as one of the main challenges. Current commercial fuel cell catalysts use platinum (Pt) NPs on a carbon black support. To reduce the amount of Pt in catalysts, bimetallic NPs of platinum, including platinum−cobalt (Pt−Co), have been tested.[58] They are found to have superior catalytic properties and use considerably less platinum.

Commercial catalysts are often produced in an initial precursor state containing the required materials in the oxide form. Transforming the catalyst precursor at elevated temperature and generally in reducing atmospheres produces the final active catalyst. During this process, the catalyst evolves into its active form by the formation of nanoparticles of specific size, composition and surface structure. The transformation of the catalyst precursor to active catalyst and the resulting nanostructures are therefore crucial to the performance of the final catalyst. However, they are not well understood in real (practical) systems as most studies have focused on "model" final catalysts. The in situ ESTEM with dynamic ED and EDX has been employed to visualize and analyze the dynamic transformation of technological bimetallic Pt−Co/C catalyst precursors containing mixed Co-oxides, Pt and Co phases, in hydrogen gas at different temperatures.[43] The catalyst precursors are reduced in the ESTEM in flowing hydrogen at 200, 450, and 700 °C, under controlled reaction conditions.[43]

No discernible changes are observed in hydrogen reduction at 200 °C, but at 450 °C nanoparticles (<3 nm) with structures of Pt, tetragonal PtCo alloys and partially ordered Pt_3Co are

https://dx.doi.org/10.1021/acs.accounts.9b00500
Acc. Chem. Res. 2020, 53, 390−399

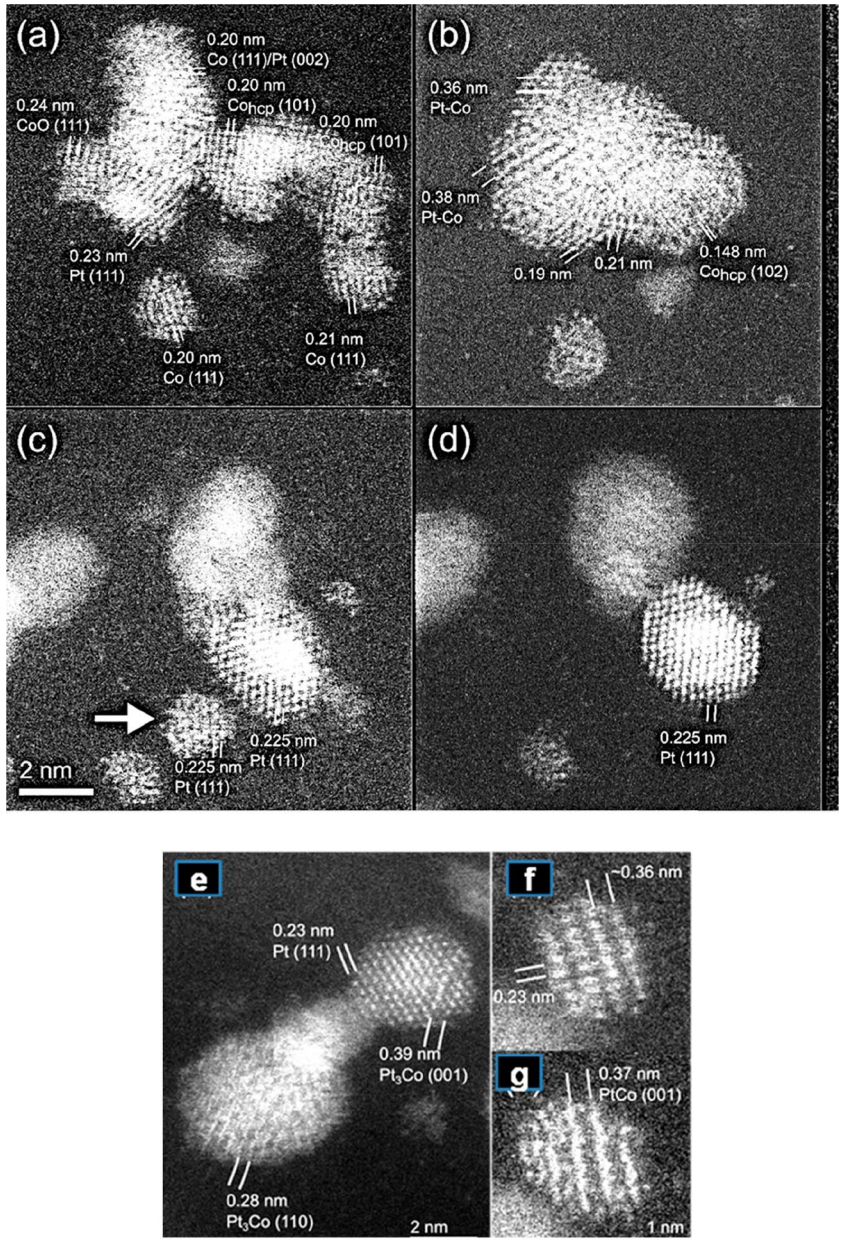

Figure 10. In situ dynamic ESTEM-HAADF of practical precursor transformation at 450 °C in hydrogen for 6 h: (a) RT; (b) the corresponding image at 450 °C in H_2, showing agglomeration and multiple phases. (c) RT and (d) disappearance of Pt cluster (indicated by arrow in (c)). (Scale bar = 2 nm.) Alloy structures at higher magnifications: (e) Pt_3Co and (f,g) PtCo NP rotating between (f) and (g). Frames (f) and (g) are 2 and 3 h into the reaction, respectively.

present. Following the reduction at 700 °C, ordered Pt_3Co and PtCo NPs larger than 4 nm are observed and the average nanoparticle size is almost tripled relative to the fresh precursor. In the reduction at 700 °C, many of the smaller NPs including Pt NPs are observed to disappear, suggesting Ostwald ripening.[43] The in situ observations reveal the nature of the complex catalyst precursor transformation at the atomic level and the creation of bimetallic PtCo fuel cell catalysts with multiple phases.

Dynamic ESTEM-HAADF images in hydrogen reaction for 6 h at 450 °C, shown in Figure 10, illustrate particle coarsening and alloy structures at the atomic level.

CONCLUSIONS AND OUTLOOK

We have presented visualization and analysis of single atom dynamics and atomic scale reaction mechanisms of nanocatalysts of interest in energy and fuel cells, and of redox and regeneration of catalysts, using ESTEM under controlled reaction conditions. The dynamic ESTEM observations reveal the evolution of single atoms, the formation of atom clusters, and the resulting faceting in irregular nanoparticles, and that the primary role of irregular nanoparticles is to act as reservoirs of low coordinated atoms and clusters. The minimization of the particle surface energy is the fundamental driver for this process. The results provide a better understanding of the role of nanoparticles. Collectively, the single atom resolution ESTEM findings generate new structural insights into catalyst dynamics important in optimizing chemical reactions and

https://dx.doi.org/10.1021/acs.accounts.9b00500
Acc. Chem. Res. 2020, 53, 390−399

developing improved catalysts and processes. The ESTEM is opening up new opportunities for observing and understanding single atom dynamics in many chemical reactions.

AUTHOR INFORMATION

Corresponding Authors

Edward D. Boyes − *The York Nanocentre, Department of Physics, and Department of Electronic Engineering, University of York, York YO10 5DD, United Kingdom;* orcid.org/0000-0001-8456-1208; Email: ed.boyes@york.ac.uk

Pratibha L. Gai − *The York Nanocentre, Department of Physics, and Department of Chemistry, University of York, York YO10 5DD, United Kingdom;* orcid.org/0000-0003-3837-7148; Email: pratibha.gai@york.ac.uk

Authors

Alec P. LaGrow − *The York Nanocentre and Department of Physics, University of York, York YO10 5DD, United Kingdom;* orcid.org/0000-0002-3306-6458

Michael R. Ward − *The York Nanocentre and Department of Physics, University of York, York YO10 5DD, United Kingdom*

Robert W. Mitchell − *The York Nanocentre and Department of Physics, University of York, York YO10 5DD, United Kingdom*

Complete contact information is available at: https://pubs.acs.org/10.1021/acs.accounts.9b00500

Notes

The authors declare no competing financial interest.

Biographies

Edward Boyes, PhD Cambridge, Senior Research Fellow at Oxford and Fellow Wolfson College, Oxford; DuPont Company CR&D (USA) and Technical Advisory Group President's Council of Advisors on Science and Technology for reviews of National Nanotechnology Initiative (NNI); Professor of Physics and Electronics, and founding Co-Director, The York Nanocentre, University of York (UK).

Alec P. LaGrow earned his Ph.D. from Victoria University of Wellington in 2012. He worked as a postdoctoral research associate at King Abdullah University of Science and Technology, University of York and University College London. He is currently a Facility Manager in Electron Microscopy at the International Iberian Nanotechnology Laboratory, Braga, 4715-330, Portugal.

Michael R Ward gained his PhD from the University of York in 2013 where he continued as a postdoctoral research associate. At York, he focused on in situ ESTEM studies of nanoparticle and atomically dispersed catalysts. He is currently a materials scientist at the National Nuclear Laboratory specializing in postirradiation evaluation.

Robert W. Mitchell gained his PhD from the University of York. He served as a postdoctoral research associate at the York Nanocentre in the Boyes and Gai group. At York, he focused on in situ E(S)TEM studies of Fischer−Tropsch catalysis.

Pratibha Gai is a Fellow of the Royal Society and the Royal Academy of Engineering. She is Professor and Chair of Electron Microscopy in Departments of Chemistry and Physics, and founding Co-Director of the York Nanocentre at University of York, UK. Previously she held senior positions as DuPont research fellow and concurrently as adjunct Professor at University of Delaware and led the In Situ Electron Microscopy and Catalysis Group at University of Oxford, after obtaining her PhD in physics from University of Cambridge.

ACKNOWLEDGMENTS

The work was supported by EPSRC (UK) Research Grant EP/J0118058/1.

REFERENCES

(1) van Santen, R. A. *Heterogeneous Catalysis: from principles to applications*; Beller, M., Renken, A., van Santen, R., Eds.; Wiley-VCH Verlag: Weinheim, 2012; p 113−151.

(2) Crespo-Quesada, M.; Yarulin, A.; Jin, M.; Xia, Y.; Kiwi-Minsker, L. Structure Sensitivity Of Alkynol Hydrogenation On Shape- And Size-Controlled Palladium Nanocrystals: Which Sites are most Active and Selective? *J. Am. Chem. Soc.* **2011**, *133*, 12787−12794.

(3) Haruta, M.; Kobayashi, T.; Sano, H.; Yamada, N. Novel Gold Catalysts for The Oxidation Of Carbon-Monoxide at a Temperature Below 0 C. *Chem. Lett.* **1987**, *16*, 405−408.

(4) Boyes, E. D.; Gai, P. L. Environmental High Resolution Electron Microscopy and Applications to Chemical Science. *Ultramicroscopy* **1997**, *67*, 219−232.

(5) Gai, P. L.; Kourtakis, K. Solid state defect mechanism in vanadyl pyrophoshate: implications for selective oxidation. *Science* **1995**, *267*, 661−663.

(6) Gai, P. L. Direct Probing of Gas Molecule-Solid Catalyst Interactions on the Atomic Scale. *Adv. Mater.* **1998**, *10*, 1259−1263.

(7) Gai, P. L.; Boyes, E. D. *Electron Microscopy in Heterogeneous Catalysis*; IOP Publishers: Bristol, UK and Philadelphia, 2003.

(8) Gai, P. L.; Boyes, E. D. Atomic resolution ETEM. In *Handbook of Nanoscopy*; Van Tendeloo, G., Van Dyck, D., Pennycook, S., Eds.; Wiley-VCH: Germany, 2012; Vol. *1*, pp 375−403.

(9) Haggin, J. In situ electron microscopy technique probes catalysis at atomic level. *Chem. Eng. News* **1995**, *73*, 39−41.

(10) Liu, L.; Corma, A. Metal catalysts for heterogeneous catalysts, from single atoms to nanoclusters and nanoparticles. *Chem. Rev.* **2018**, *118*, 4981−5079.

(11) Herzing, A. A.; Kiely, C. J.; Carley, A. F.; Landon, P.; Hutchings, G. J. Identification of Active Gold Nanoclusters on Iron Oxide Supports for CO Oxidation. *Science* **2008**, *321*, 1331−1335.

(12) Heiz, U.; Sanchez, A.; Abbet, S.; Schneider, W. D. Catalytic Oxidation of carbon Monoxide on Monodispersed Platinum Clusters: each Atom Counts. *J. Am. Chem. Soc.* **1999**, *121*, 3214−3217.

(13) Lei, Y.; Mehmood, F.; Lee, S.; Greeley, J.; Lee, B.; Seifert, S.; Winans, R. E.; Elam, J. W.; Meyer, R. J.; Redfern, P. C.; Teschner, D.; Schlogl, R.; Pellin, M. J.; Curtiss, L. A.; Vajda, S. Increased silver activity for direct propylene epoxidation via subnanometer size effects. *Science* **2010**, *328*, 224−228.

(14) Turner, M.; Golovko, V. B.; Vaughan, O. P. H.; Abdulkin, P.; Berenguer-Murcia, A.; Tikhov, M. S.; Johnson, B. F. G.; Lambert, R. M. Selective Oxidation with Dioxygen by Gold Nanoparticle Catalysts derived from 55-Atom Clusters. *Nature* **2008**, *454*, 981−983.

(15) Kaden, W. E.; Wu, T.; Kunkel, W. A.; Anderson, S. L. Electronic Structure Controls Reactivity of Size-Selected Pd Clusters Adsorbed on TiO_2Surfaces. *Science* **2009**, *326*, 826−829.

(16) Qiao, B.; Wang, A.; Yang, X.; Allard, L. F.; Jiang, Z.; Cui, Y.; Liu, J.; Li, J.; Zhang, T. Single-atom catalysis of CO oxidation using Pt1/FeOx. *Nat. Chem.* **2011**, *3*, 634−641.

(17) Thomas, J.; Saghi, Z.; Gai, P. L. Can a single atom serve as the active site in some heterogeneous catalysts? *Top. Catal.* **2011**, *54*, 588−594.

(18) Yang, X. F.; Wang, A.; Qiao, B.; Li, J.; Liu, J.; Zhang, T. Single atom catalysts: a new frontier in heterogeneous catalysis. *Acc. Chem. Res.* **2013**, *46*, 1740−1748.

(19) Hansen, T. W.; DeLaRiva, A. T.; Challa, S. R.; Datye, A. K. Sintering of Catalytic Nanoparticles: Particle Migration or Ostwald Ripening? *Acc. Chem. Res.* **2013**, *46*, 1720−1730.

(20) Crewe, A. V.; Wall, J.; Langmore, J. Visibility of Single Atoms. *Science* **1970**, *168*, 1338−1341.

(21) Batson, P. E.; Dellby, N.; Krivanek, O. L. Sub-Ångstrom Resolution using Aberration Corrected Electron Optics. *Nature* **2002**, *418*, 617−620.

(22) Allard, L. F.; Flytzani, M.; Overbury, S. H. Behavior of Au species in Au/FeOx catalysts characterized by heating techniques, and aberration-corrected STEM imaging. *Microsc. Microanal.* **2010**, *16*, 375−385.
(23) Howie, A. Image Contrast and Localized Signal Selection Techniques. *J. Microsc.* **1979**, *117*, 11−23.
(24) Gai, P. L.; Lari, L.; Ward, M. R.; Boyes, E. D. Visualiation of Single Atom Dynamics and their Role in Nanocatalysis under Controlled Reaction Environments. *Chem. Phys. Lett.* **2014**, *592*, 355−359.
(25) Haider, M.; Uhlemann, S.; Schwan, E.; Rose, H.; Kabius, B.; Urban, K. Electron Microscopy Image Enhanced. *Nature* **1998**, *392*, 768−769.
(26) Gai, P. L.; Boyes, E. D.; Hansen, P.; Helveg, S.; Giorgio, S.; Henry, C. Atomic Resolution Environmental Transmission Electron Microscopy for Probing Gas-Solid Reactions in Heterogeneous Catalysis. *MRS Bull.* **2007**, *32*, 1044−1048.
(27) Crozier, P.; Wang, R.; Sharma, R. In situ Environmental TEM Studies of Dynamic Changes in Cerium-Based Oxide Nanoparticles During Redox Processes. *Ultramicroscopy* **2008**, *108*, 1432−1440.
(28) Simonsen, S. B.; Dahl, S.; Johnson, E.; Helveg, S. Ceria catalyzed soot oxidation studied by environmental transmission electron microscopy. *J. Catal.* **2008**, *255*, 1−5.
(29) Pattinson, S.; Diaz, R. E.; Stelmashenko, N.; Windle, A. H.; Ducati, C.; Stach, E. A.; Koziol, K. In Situ Observation of the Effect of Nitrogen on Carbon Nanotube Synthesis. *Chem. Mater.* **2013**, *25*, 2921−2923.
(30) Yoshida, H.; Takeda, S.; Uchiyama, T.; Kohno, H.; Homma, Y. Atomic-scale in-situ observation of carbon nanotube growth from solid state iron carbide nanoparticles. *Nano Lett.* **2008**, *8*, 2082−2086.
(31) Hansen, T. W.; Wagner, J. Environmental Transmission Electron Microscopy. *Microsc. Microanal.* **2012**, *18*, 684−690.
(32) Li, Y.; Li, Y.; Sun, Y.; Butz, B.; Yan, K.; Koh, A.; Zhao, J.; Pei, A.; Cui, Y. Revealing Nanoscale Passivation and Corrosion Mechanisms of Reactive Battery Materials in Gas Environments. *Nano Lett.* **2017**, *17*, 5171−5178.
(33) Yoshida, K.; Bright, A. N.; Ward, M. R.; Lari, L.; Zhang, X.; Hiroyama, T.; Boyes, E. D.; Gai, P. L. Dynamic Wet-ETEM Observation of Pt/C Electrode Catalysts in a Moisturized Cathode Atmosphere. *Nanotechnology* **2014**, *25*, 425702.
(34) Gai, P. L.; Boyes, E. D. Advances in In-Situ Atomic Resolution-Environmental Transmission Electron Microscopy (ETEM) and 1ÅngstromAberration Corrected Electron Microscopy. *Microsc. Res. Tech.* **2009**, *72*, 153−164.
(35) Boyes, E. D.; Ward, M. R.; Lari, L.; Gai, P. L. ESTEM imaging of single atoms under controlled temperature and gas environment conditions in catalyst reaction studies. *Ann. Phys. (Berlin, Ger.)* **2013**, *525*, 423−429.
(36) Boyes, E. D.; Gai, P. L. Visualising Reacting Single Atoms under Controlled Conditions: Advances in Atomic Resolution In-situ Environmental (Scanning) Transmission Electron Microscopy (E(S)TEM). *C. R. Phys.* **2014**, *15*, 200−213.
(37) Boyes, E. D.; Gai, P. L. Visualizing Reacting Single Atoms in Chemical Reactions: Advancing the Frontiers of Materials Research. *MRS Bull.* **2015**, *40*, 600−604.
(38) LaGrow, A. P.; Ward, M. R.; Lloyd, D. C.; Gai, P. L.; Boyes, E. D. Visualizing the Cu/Cu2O Interface Transition in Nanoparticles with Environmental Scanning Transmission Electron Microscopy (ESTEM). *J. Am. Chem. Soc.* **2017**, *139*, 179−185.
(39) LaGrow, A. P.; Lloyd, D. C.; Gai, P. L.; Boyes, E. D. In Situ Scanning Transmission Electron Microscopy of Ni Nanoparticle Redispersion via the Reduction of Hollow NiO. *Chem. Mater.* **2018**, *30*, 197−203.
(40) Gai, P. L.; Yoshida, K.; Ward, M. R.; Walsh, M.; van de Water, L.; Baker, R. T.; Watson, M. J.; Boyes, E. D. Visualisation of Single Atom Dynamics in Water Gas Shift Reaction for Hydrogen Generation. *Catal. Sci. Technol.* **2016**, *6*, 2214−2227.
(41) Somorjai, G.; York, R. L.; Butcher, D.; Park, J. Y. The evolution of model catalytic systems; studies of structure, bonding and dynamics from single crystal metal surfaces to nanoparticles, and from low pressure (<10−3 Torr) to high pressure (10−3 Torr). *Phys. Chem. Chem. Phys.* **2007**, *9*, 3500−3513.
(42) Koch, C. T. Quantitative STEM. PhD Thesis, Arizona State University, Tempe, AZ, 2002.
(43) Ward, M. R.; Theobald, B.; Sharman, J.; Boyes, E. D.; Gai, P. L. Direct observations of Dynamic PtCo Interactions in Fuel Cell Catalyst Precursors at the Atomic level using E(S)TEM. *J. Microsc.* **2018**, *269*, 143−150.
(44) Mitchell, R. W.; Lloyd, D. C.; van de Water, L.G. A.; Ellis, P. R.; Metcalfe, K. A.; Sibbald, C.; Davies, L. H.; Enache, D. I.; Kelly, G. J.; Boyes, E. D.; Gai, P. L. Effect of Pretreatment Method on The Nanostructure and Performance of Supported Co Catalysts in Fischer−Tropsch synthesis. *ACS Catal.* **2018**, *8*, 8816−8829.
(45) Fischer, F.; Tropsch, H. Process for the production of paraffinhydrocarbons with more than one atom. US Patent US 1746464 A, 1925.
(46) King, D. L.; De Klerk, A. Overview of Feed-to-Liquid (XTL) Conversion. *ACS Symp. Ser.* **2011**, *1084*, 1−24.
(47) Iglesia, E. Design, Synthesis, and Use of Cobalt-Based Fischer−Tropsch Synthesis Catalysts. *Appl. Catal., A* **1997**, *161*, 59−78.
(48) Wolters, M.; Munnik, P.; Bitter, J. H.; de Jongh, P. E.; de Jong, K. P. How NO Affects Nickel and Cobalt Nitrates at Low Temperatures to Arrive at Highly Dispersed Silica-Supported Nickel and Cobalt Catalysts. *J. Phys. Chem. C* **2011**, *115*, 3332−3339.
(49) Enache, D. I.; Rebours, B.; Roy-Auberger, M.; Revel, R. In Situ XRD Study of the Influence of Thermal Treatment on the Characteristics and the Catalytic Properties of Cobalt-Based Fischer−Tropsch Catalysts. *J. Catal.* **2002**, *205*, 346−353.
(50) Brittman, S.; Yoo, Y.; Dasgupta, N. P.; Kim, S.-i.; Kim, B.; Yang, P. Epitaxially Aligned Cuprous Oxide Nanowires for All-Oxide, Single-Wire Solar Cells. *Nano Lett.* **2014**, *14*, 4665−4670.
(51) Gai, P. L.; Smith, B. C.; Owen, G. Bulk Diffusion of Metal Particles on Ceramic Substrates. *Nature* **1990**, *348*, 430−432.
(52) LaGrow, A. P.; Lloyd, D. C.; Schebarchov, D.; Gai, P. L.; Boyes, E. D. In Situ Visualization of Site-Dependent Reaction Kinetics in Shape-Controlled Nanoparticles: Corners vs Edges. *J. Phys. Chem. C* **2019**, *123*, 14746−14753.
(53) Wagner, J. B.; Hansen, P. L.; Molenbroek, A. M.; Topsøe, H.; Clausen, B. S.; Helveg, S. In situ spectroscopy studies of gas-dependent metal-support interactions in Cu/ZnO catalysts. *J. Phys. Chem. B* **2003**, *107*, 7753.
(54) Martin, T. E.; Gai, P. L.; Boyes, E. D. Dynamic Imaging of Ostwald Ripening by Environmental Scanning Transmission Electron Microscopy. *ChemCatChem* **2015**, *7*, 3705−3711.
(55) Simonsen, S. B.; Chorkendorff, I.; Dahl, S.; Skoglundh, M.; Sehested, J.; Helveg, S. Direct Observations of Oxygen-induced Platinum Nanoparticle Ripening studied by In Situ TEM. *J. Am. Chem. Soc.* **2010**, *132*, 7968−7975.
(56) van den Berg, R.; Parmentier, T. E.; Elkjær, C. F.; Gommes, C. J; Sehested, J.; Helveg, S.; de Jongh, P. E.; de Jong, K. P. Support Functionalization to Retard Ostwald Ripening in Copper Methanol Synthesis Catalysts. *ACS Catal.* **2015**, *5*, 4439−4448.
(57) Gai, P. L.; Kourtakis, K.; Coulson, D. R.; Sonnichsen, G. C. Microstructural Studies on the Effect of Steam Exposure and Cation Promoters on Vanadium Phosphorus Oxides: New Correlations with n-Butane Reaction Chemistry. *J. Phys. Chem. B* **1997**, *101*, 9916−9925.
(58) Chen, S.; Ferreira, P. J.; Sheng, W. C.; Yabuuchi, N.; Allard, L. F.; Shao-Horn, Y. Enhanced Activity for Oxygen Reduction Reaction on "Pt(3)Co" Nanoparticles: Direct evidence of percolated and sandwich-segregation structures. *J. Am. Chem. Soc.* **2008**, *130*, 13818−13819.

https://dx.doi.org/10.1021/acs.accounts.9b00500
Acc. Chem. Res. 2020, 53, 390−399